TECHNICAL NOTES

NATIONAL ADVISORY COMMITTEE FOR AERONAUTICS

No. 595

BENDING TESTS OF CIRCULAR CYLINDERS OF CORRUGATED ALUMINUM-ALLOY SHEET

By Alfred S. Niles, John C. Buckwalter, and Warren D. Reed
Stanford University

Washington
March 1937

NATIONAL ADVISORY COMMITTEE FOR AERONAUTICS

TECHNICAL NOTE NO. 595

BENDING TESTS OF CIRCULAR CYLINDERS OF CORRUGATED ALUMINUM-ALLOY SHEET

By Alfred S. Niles, John C. Buckwalter, and Warren D. Reed

SUMMARY

Bending tests were made of two circular cylinders of corrugated aluminum-alloy sheet. In each test failure occurred by bending of the corrugations in a plane normal to the skin. It was found, after analysis of the effect of short end bays, that the computed stress on the extreme fiber of a corrugated cylinder is in excess of that for a flat panel of the same basic pattern and panel length tested as a pin-ended column. It is concluded that this increased strength was due to the effects of curvature of the pitch line. It is also concluded from the tests that light bulkheads closely spaced strengthen corrugated cylinders very materially.

The section properties of corrugated sheet are summarized in an appendix.

INTRODUCTION

The earliest stressed-skin metal airplanes, those of Dr. Junkers, were constructed with corrugated duralumin covering. Some designers have followed Dr. Junkers' lead in this respect, while others have used a smooth skin reinforced by various types of stiffeners. Although some early studies of the problem of the design of stressed-skin airplanes indicated that the highest strength-weight ratios could be obtained by the use of corrugated covering, the value of these studies was largely vitiated by lack of knowledge of the actual strength of either the corrugated skin or the smooth skin with stiffeners. As a consequence, numerous tests have been made to obtain the experimental data needed as the foundation for satisfactory methods of designing both types of stressed skin.

The great majority of the test data that have so far been generally available to designers have pertained to the use of smooth skin, as the corrugated material lost favor on account of the tailoring difficulties encountered in its use. Recently a number of designers have shown a renewed interest in the use of corrugated sheet, and it appears desirable to make a study of this material.

In reference 1 are published the results of an extensive study of the compressive strength of flat panels of corrugated sheet in which failure occurs by local buckling of the corrugations. It is shown in reference 1 that when local failure does not occur, the compressive strength of a corrugated panel is given by the column curve for the material.

When corrugated sheet is used in stressed-skin structures for aircraft, the pitch line is usually curved. The purpose of this report is to present the results of bending tests made of two corrugated cylinders at Stanford University during the winter of 1930-31. (A preliminary report of these results is contained in a Stanford University thesis by Buckwalter and Reed entitled "Bending Tests on Corrugated Aluminum-Alloy Cylinders." These tests were similar to those made by Mossman and Robinson on cylinders with smooth skin (reference 2).

DESCRIPTION OF TEST CYLINDERS

The two cylinders, constructed of aluminum alloy heat-treated to the specifications of the U. S. Army Air Corps, were furnished by the Douglas Aircraft Company. As originally furnished, they were identical in every respect except in the number and spacing of the bulkhead rings. The bulkhead rings were located so that in cylinder 1 the critical bay was 18 inches in length and in cylinder 3 it was 9 inches. The length of each cylinder was 36 inches, and the diameter of the pitch line of the corrugated covering was the same. The covering consisted of a corrugated sheet of a standard Douglas Company section having a nominal pitch of 1.25 inches and a depth of 0.50 inch, with a thickness of 0.022 inch. Only one longitudinal seam was necessary in each specimen and it was made by nesting corrugations and riveting along the node. The bulkhead rings were of open "hat" section of the same shape and size as those used in the smooth-skin cylinders

tested by Mossman and Robinson and reported in reference 2. At each end of the cylinders an inner and an outer angle ring was riveted to the inner and outer nodes of the corrugations, respectively, and the outstanding legs of these angles carried the bolts that attached the cylinders to the parts of the test jig. These angles were 11/16 by 15/16 by 0.064 inch section. The general construction of these specimens can be seen very well from figures 1 to 4, which are photographs of them after failure.

In the design of the cylinders it was realized that the restraint imposed on the sheet at the ends of the cylinders by bolting the end rings to parts of a rigid test jig would be greater than that at the intermediate bulkheads. If failure occurred in the bay adjacent to the end rings, this restraint at one end of the critical panel would probably cause the stress at failure to be in excess of what might be expected for sheet in a continuous structure. Hence, it was desired that the failure in the specimens would take place in a central panel where the end restraint would not be such an important factor. In order to accomplish this aim, cylinder 1 had a bulkhead ring located 9 inches from each end, leaving an 18-inch bay in the middle in which failure was almost certain to occur. Cylinder 2 had three equally spaced bulkheads, which divided the specimen into four 9-inch bays. The second bay from one end was expected to be the critical one, and it proved to be so.

Based on the nominal dimensions, the section characistics of the corrugated sheet were as follows:

Pitch/depth ratio, $p/d = 1.25/0.5$	2.50
Ratio of the radius of corrugations to thickness, $r/t = 0.3235/0.022$	14.70
Weight ratio for p/d of 2.50 (fig. A-1) ..	1.40
Radius of gyration, ρ (fig. A-1) = 0.355×0.5	0.1775

Experience has shown that commercial corrugated material is seldom true to nominal dimensions, the allowable manufacturing practices and tolerances permitting an appreciable variation between nominal and actual dimensions. After the bending tests had been completed, therefore, a

section was cut from each cylinder to permit more accurate determinations of thickness of material, equivalent thickness of flat sheet, radius of gyration of a corrugation, and r/t ratio.

The actual thickness of the material used was determined by direct measurement with micrometer calipers with small spherical-ended jaws. For the determination of the equivalent thickness of flat sheet, the sections were trimmed to a rectangular shape with two sides along troughs of corrugations and at a distance from each other of about six times the pitch. The other sides were normal to the corrugations. These pieces were held by hand against a flat surface and the projected area was measured. They were then weighed. The weights divided by the projected area and the density of the material gave what were considered the more reliable values for the equivalent thicknesses. The radius of gyration of a corrugation and the r/t ratio were obtained by direct measurement of the pitch and depth of the corrugations, both with the sections curved, as when first cut from the cylinders, and while pressed against a flat surface. Although it was difficult to measure the pitch precisely, particularly with the pitch line curved, it is believed that the error is less than the noted variation between corrugations. The radius of gyration was computed from the pitch-depth ratio assuming the section to be made up of perfectly circular arcs tangent at the pitch line, using for the purpose the curves of appendix I. The radius of curvature of a corrugation r, was also computed from the pitch-depth ratio on the same assumption, using the formula derived in appendix I. Finally, the equivalent thickness was computed from the measured thickness, the weight ratio for the observed pitch-depth ratio, and the curve of figure A-1. The equivalent thicknesses obtained in this manner were smaller than those obtained by weighing and, as they were not considered as reliable as the latter, were not used in the analysis of the cylinder tests.

The measurements and computations made in this study are recorded in table I.

TABLE I

DETERMINATION OF PROPERTIES OF CORRUGATED SHEET

Item	How obtained	Cylinder 1	Cylinders 2 and 3
1. Actual thickness, in.	Direct measurement	0.0215	0.023
2. Length of section, in.	Direct measurement	5.83	3.96
3. Width of section, in.	Direct measurement	7.63	7.76
4. Projected area, sq.in.	(2) × (3)	44.5	30.3
5. Weight, g	Direct measurement	57.6	41.5
6. Weight, g/sq.in.	(5)/(4)	1.29	1.37
7. Weight, lb./sq.in.	(6) × 0.00220	.00284	.00302
8. Equivalent thickness, in.	(7)/0.1011	.0284	.0299
9. Pitch p, in.	Direct measurement	1.28	1.28
10. Depth d, in.	Direct measurement	.41	.41
11. Pitch/depth, p/d	(9)/(10)	3.12	3.12
12. ρ/d	Figure A-1	.359	.359
13. Radius of gyration ρ, in.	(10) × (12)	.147	.147
14. Weight ratio	Figure A-1	1.26	1.26
15. Equivalent thickness, in.	(1) × (14)	.0271	.0290
16. Radius of corrugations r, in.	Appendix I	.349	.349
17. r/t	(16)/(1)	16.2	15.2

For the purpose of computing the stresses in bending it was assumed that the actual cylinders would have the same moments of inertia and section moduli as cylinders of 36-inch diameter covered with smooth skin of thicknesses equal to the equivalent thicknesses of line 8 in table I. The properties of this equivalent cylinder and the slenderness ratios of a single corrugation in the critical panels were then computed as shown in table II.

TABLE II

COMPUTATION OF SECTION MODULI AND SLENDERNESS RATIOS

Item	Reference	Cylinder 1	Cylinders 2 and 3
Equivalent thickness t', in.	Table I, line 8	0.0284	0.0298
Diameter, D, in.	-	36	36
Moment of inertia, $in.^4$	$I = 0.\pi 94\ t'D^3$	521	546
Section modulus, $in.^3$	I/R	29.0	30.5
Length of bay, in.	-	18	9
Radius of gyration, ρ, in.	-	.147	.147
Slenderness ratio ...	L/ρ	122.4	61.2

DESCRIPTION OF TEST SET-UP

The test jig was arranged as shown in figures 5 to 8. The main jig consisted of a backplate A (figs. 5 and 8) bolted to two horizontal structural steel channels B and braced to them by two pieces of conduit pipe C. An H-beam D was bolted to the base channels and rested on the weighing table of a testing machine. A wooden structure E supported the backplate end of the jig and held the base

channels in a horizontal position. The tetrapod unit consisted of a structural steel angle F bent into a ring and welded at the joint, to which was bolted two steel-strap tension members G and two pieces of conduit pipe H for compression members. The tension and compression members were welded at the apex I into a fitting to which the load was applied from the head of the testing machine through a link J.

Each specimen was bolted to the backplate and to the tetrapod ring with 10-24 roundhead machine screws. These screws were put through the outstanding legs of the angle rings, a screw opposite each trough of the corrugation over three-quarters of the circumference on the tension side, and opposite every other trough on the compression side. The longitudinal joint in the corrugated sheet was placed at the top of the cylinder where it would be in tension and would be least apt to influence failure. Shims of sheet iron were used where necessary between the specimen and the jig parts so that tightening of the machine screws would not cause strain in the cylinder. A Riehle Bros. motor-driven testing machine of 30,000 pounds capacity was used to supply the load.

As the testing-machine head moved down, a vertical load was applied to the apex I and bending and shear forces were set up in the test specimen. Since member D was directly under the point of application of the load, the latter could be measured directly on the scale beam of the machine, the jig acting in the fashion of a nutcracker with force and reaction applied at I and D, respectively.

An attempt was made to measure the elongations and compressions of the most stressed fibers of the cylinders by the use of extensometers. The arrangement used, however, proved to be unsatisfactory because any slight bulging of the sheet caused an angular movement of the extensometer mounting, which prevented the extensometer readings from being true measures of the deformation of the specimen.

Readings were also taken of the change in length of the vertical diameter of a bulkhead ring using the same instrument as had been employed for the purpose by Mossman and Robinson (reference 2).

TEST PROCEDURE

The procedure of testing consisted in the application of the load in desired increments to the apex of the tetrapod and the noting of certain observations for each load increment. These observations are indicated by letter and numeral in the log sheet of test 1. (See appendix II.) For each load increment, measured on the scale of the testing machine, readings were taken on the four extensometers and on the diameter gage, the beam deflections A and B were measured, and the formation of bulges was observed at points on the specimen indicated by the roman numerals.

The tetrapod unit, weighing 310 pounds, was the first load to be applied to the specimen. Since its point of application was at the center of gravity of the unit instead of at the apex, the equivalent load at the apex was determined and is included in the log sheets. It is simply a fictitious load giving the same moment at the critical section of the specimen as the 310-pound load of the tetrapod. All subsequent load increments were applied through the head of the testing machine to the apex.

After the first maximum load was reached, the load applied by the testing machine was entirely removed and then reapplied to a second maximum value in order to determine the strength of the specimen after failure had occurred.

RESULTS OF TESTS

A complete record of the first and third tests is contained in appendix II; the important results of all three tests are summarized in table III. A rough mental picture of the progress of each test may be formed from the notes in the last column of the log sheets.

TABLE III

SUMMARY OF TEST RESULTS

Test	Cylinder	Bulkhead ring spacing in.	Weight lb.	L/ρ of critical panel	Section modulus	Maximum moment in.-lb.	Maximum shear lb.	Maximum f_b lb./sq.in.
1	1	18	18.6	122.4	29.0	525,520	5,300	18,100
2	2	9	20.0	61.2	30.5	828,630	7,910	27,150
3	3	9	25.3	61.2	30.5	866,110	8,260	28,400

The results of test 2 are of no direct importance in this investigation, since the cylinder failed by tearing of the sheet from the rivets in the end rings on the tension side before definite failure occurred on the compression side. These rivets had imperfect heads adjacent to the corrugated sheet, resulting from the difficulty of getting a head-forming tool between the two end rings during fabrication. The specimen was returned to the Douglas Company where the weak section was reinforced. The repaired cylinder was designated cylinder 3. The excess weight of cylinder 3 over cylinder 2 was due entirely to the reinforcement of the latter, a measure that would have been unnecessary had it been possible to form better rivets. Consequently, it seems only fair to assume that the maximum stress found from test 3 could have been obtained with a specimen weighing no more than cylinder 2, which is the same as the weight of cylinder 1 plus the weight of an additional bulkhead ring.

Cylinders 1 and 3, after failure, are shown in figures 1 to 4. It is evident from these pictures that the corrugated sheet in the critical bays behaved in the manner of a column. Final failure occurred in the vicinity of the first bulges to form, the bulges gradually increasing with load until the sheet buckled. In both specimens this buckling at the middle of the panel was accompanied by buckling or cracking of the sheet over the bulkheads at each end of the critical bay. As shown in figure 4, cylinder 3 failed by buckling inward on one side of the vertical axis of the specimen, and outward on the other, while the corrugation at the axis remained practically straight. As noted in the log sheet, before any load was applied,

very slight initial bulges in the specimen, corresponding in location and direction to the final ones, were observed, and the peculiar pattern of failure evidently resulted from the gradual growth of these initial bulges. They were no more pronounced, however, than bulges which might be expected to appear in any practical structure of the corrugated monocoque type.

No consideration has been given to the readings of gages 1 to 4 because observation during test showed them to be unreliable. They were omitted entirely in test 3.

Gage 5, indicating the change in length of the vertical axis of the first bulkhead out from the backplate, gave rather interesting results. For the first test it showed a maximum increase in the axis of 0.028 inch, and for the second, a decrease of 0.019 inch. The fact that in one case the axis elongated while in the other it contracted may possibly be explained by the presence, in the first, of a tendency of the sheet in the critical panel to bulge outward at the bottom, thus tending to stretch the vertical axis, while in the second, the main bulging was inward, tending to shorten the axis. Unfortunately, this gage was not used in the third test, in which the bulges were in opposite directions on either side of the vertical axis. In this case, if the foregoing explanation is correct, one would expect no change in the length of the axis, but this fact cannot be verified. The rigid backplate and tetrapod ring undoubtedly played a large part in maintaining the original shape of the intermediate rings under load and without this influence the deflections noted might have been entirely different. Gage 5 therefore gives no indication of what deflections might be expected in the bulkhead rings of a monocoque structure with no solid bulkheads but shows, merely, what occurred in these particular tests.

After complete failure of cylinders 1 and 3, the load was entirely removed, except for the weight of the tetrapod, and then reapplied to determine the strength after failure. As noted in the logs, cylinder 1 carried 67 percent of the original load and cylinder 3 carried 77.2 percent.

As it seemed desirable to determine the compressive strength for local failure of the corrugated section used, small panels were cut from each cylinder and tested in compression. Two such panels were cut from cylinder 1, each with a length parallel to the corrugations of approx-

imately 2.8 inches, and one with a length of approximately 3.6 inches from cylinder 3. All three panels had a width of six complete corrugations. The free edges of these panels were reinforced by bending them about a small radius. The panels were then tested in compression with flat ends. In spite of the fact that the reinforcement of the free edges was not sufficient to prevent failure starting at those locations, and that the tests were not made with any great care, both panels from cylinder 1 showed ultimate strengths of 34,000 pounds per square inch or more. That from cylinder 3 did not have failure start at the free edges and did not fail until the stress was 38,000 pounds per square inch.

DISCUSSION OF TEST RESULTS

A corrugated sheet under compression will fail either by bending normal to the plane of the sheet or by local buckling of the corrugations, depending upon which gives the lower strength. In the panel tests mentioned in the preceding paragraph it was found that the strength for local failure was in excess of 34,000 pounds per square inch. As the cylinders failed at computed stresses of 28,400 pounds per square inch and less (table III), it is concluded that failure in the cylinders occurred by bending of the corrugations normal to the skin. This conclusion is also verified by the observed types of failure. (See figs. 1 to 4.)

It would be desirable to compare the strengths developed in the cylinder tests with those developed in tests of small panels with curved pitch line but no adequate panel data are available, because of the great difficulty of obtaining proper end conditions for bending failure of the corrugations in a panel with curved pitch line. If, however, the cylinder test data be compared with the data on compressive tests of corrugated panels with straight pitch lines, some very interesting relationships are to be found.

DETERMINATION OF INDICATED RESTRAINT COEFFICIENTS FROM TESTS

Since the failures were due to bending rather than to local instability of the corrugations, the first step in comparing the results of the cylinder tests with those to be expected from compression tests of flat panels is to plot the computed stresses at failure against the ratios of the length of the critical bay to the radius of gyration of a single corrugation. Such a method was used to obtain figure 9. For convenience, the column curves for aluminum alloy for $c = 1$, $c = 2$, and $c = 3$ are also shown in the figure.

The ultimate stresses in both tests fall within the range of the Johnson straight-line formula

$$\frac{P}{A} = 48{,}000 - \frac{400}{\sqrt{c}} \frac{L}{\rho}$$

Using the values of L/ρ from table III and substituting in this formula to compute an indicated restraint coefficient c, we find that $c = 2.68$ for the cylinder with the 18-inch bay, and $c = 1.56$ for the cylinder with all bays 9 inches in length.

Owing to the continuity of the corrugated sheet across the intermediate bulkhead rings and the rigidity of the connections to the stiff backplate and tetrapod, it was to be expected that the strength of the cylinder covering would exceed that of a straight pitch-line panel of length equal to the bulkhead spacing tested between pin ends. In other words, it was to be expected that the indicated restraint coefficients computed as just indicated would exceed 1.00. Such a great difference as that found between the indicated restraint coefficients was not expected when the cylinders were designed, though studies made after the tests show that it could have been predicted from the differences in the relative lengths of the bays in the two specimens.

THEORETICAL DETERMINATION OF INDICATED RESTRAINT COEFFICIENTS

In both cylinders the failure was due to the instability of a corrugation due to the compression resulting from the bending load on the whole specimen. This corrugation may well be thought of as a continuous beam-column supported laterally at the end rings and intermediate bulkhead rings, and also continuously along its length by the adjoining corrugations. The external loading consists of a uniformly varying axial load proportional to the distance from the point of load application on the tetrapod and such transverse loads as were brought into action by the deformation of the specimen and accidental eccentricities. Too many uncertainties are involved to permit an exact analysis to determine theoretically the load at which the corrugations in the test specimens should have failed but, by the employment of certain simplifications and assumptions, some results of value have been obtained. The method of attack used was that partly developed by Buckwalter in his original study of the cylinder tests.

The first simplification of the problem was to neglect the possible supporting effect of the adjacent corrugations. This support might have been manifested in two ways. The adjoining corrugations, being subjected to lower stresses, might have carried some of the load when the most stressed corrugation began to buckle. Secondly, when the most stressed corrugation began to deflect, circumstantial stresses may have been set up in the cylinder that would have provided it with transverse support. Although such neglect of the possible supporting effect of the adjoining corrugations is practically equivalent to assuming that the curvature of the pitch line has no direct effect on the elastic stability of the compression side of the cylinder, no alternative course appeared practicable.

The second simplification was to assume the axial load to be a constant for the entire length of the corrugation. Any attempt to assume the axial load to vary between supports would have resulted in unmanageable mathematics. Even though the axial load in each span had been assumed a constant proportional to the distance of the center of the span from the point of load application, the

extra labor of computation would have been excessive for the small resultant gain in accuracy. The qualitative effect of this assumption will be discussed later.

As the intermediate bulkhead rings are light and connected to the corrugations in a manner not well suited to transmit a couple, the corrugations were assumed simply supported at their locations. At the ends of the cylinders, the corrugations were connected to the relatively very stiff backplate and tetrapod ring by fairly rigid connections. The actual degree of restraint at these points could only be estimated. Parallel analyses were therefore made, one set in which the ends were assumed fixed and another in which they were assumed pinned. The true conditions would lie between these two assumptions. In the ordinary fuselage the pin-ended assumption probably is closer to the actual conditions as the bulkheads would not be relatively as stiff as the backplate and tetrapod ring of the test jig. In the test specimens, however, the fixed end conditions are probably the more nearly applicable.

The transverse loads acting on the corrugation due to deformation of the specimen and eccentricities were assumed to be symmetrical in the following analyses, but their magnitude and distribution were left undetermined. This method is allowable as the magnitude and distribution of transverse load has no influence on the ideal critical load of a beam-column. The assumption of symmetry greatly reduced the extent of the required computations without affecting the criterions determined for ideal critical loads. This result was checked by independent analyses in which the assumption was not made; this material is omitted from the subject report to conserve space.

It was assumed that all the supports remained on a straight line and, in the cases with fixed ends, that the tangents to the elastic curve at both ends of the corrugation formed a single straight line. In the tests, however, the cylinders as a whole were bent, so that the points of support actually fell on a curved line, and the end tangents to the elastic curve were at an angle to each other and to the axial load. These actual deflections and rotations could have been allowed for in the analyses to determine ideal critical values of L/j by the addition of appropriate terms to the three-moment equations. Such terms, however, would have had no effect on the values of L/j found critical for the various cases. The situation

is exactly analogous to that of transverse load. Although a change in transverse load will make a corresponding change in the bending moments and deflections for any given value of L/j below the critical, it will not change the critical value of L/j. The same applies to deflections of the supports and rotation of the fixed supports.

Finally, it was assumed that the geometric properties of the corrugation as listed in table I were correct. This assumption had no influence on the computed values of critical L/j but did affect the values used for I and ρ, and thus the critical stress corresponding to any given value of L/j as well as the value of L/ρ for each bay.

After the foregoing assumptions were made, the beam-column representative of the most stressed corrugation of cylinder 1 could be represented diagrammatically as in figure 10. When writing the three-moment equations for this and other cases with fixed ends, the effect of the end conditions was allowed for by assuming extra end bays of zero length and including terms with appropriate subscripts for those bays. The generalized three-moment equations for the beam-column of figure 10 can be written (reference 3, ch. XI) as follows:

($M_2 = M_3$ on account of symmetry)

$$M_0 L_0 \alpha_0 + 2M_1 L_0 \beta_0 + 2M_1 L_1 \beta_1 + M_2 L_1 \alpha_1 = k_1 \qquad (5)$$

$$M_1 L_1 \alpha_1 + 2M_2 L_1 \beta_1 + 2M_2 L_2 \beta_2 + M_2 L_2 \alpha_2 = k_2 \qquad (6)$$

k_1 and k_2 are terms that are dependent on the side load W, and need not be evaluated. Since $L_0 = 0$, the first two terms in equation (5) are zero, and the equations may be rewritten

$$(2L_1 \beta_1)M_1 + (L_1 \alpha_1)M_2 = k_1 \qquad (7)$$

$$(L_1 \alpha_1)M_1 + (2L_1 \beta_1 + 2L_2 \beta_2 + L_2 \alpha_2)M_2 = k_2 \qquad (8)$$

Equations (7) and (8) are of the form

$$a_1 x + b_1 y = c_1$$

$$a_2 x + b_2 y = c_2$$

and may be expressed in determinant form as follows:

$$x = \begin{vmatrix} c_1 & b_1 \\ c_2 & b_2 \end{vmatrix}$$

$$y = \begin{vmatrix} a_1 & c_1 \\ a_2 & c_2 \end{vmatrix}$$

Then

$$x = \frac{\begin{vmatrix} c_1 & b_1 \\ c_2 & b_2 \end{vmatrix}}{\begin{vmatrix} a_1 & b_1 \\ a_2 & b_2 \end{vmatrix}} = \frac{c_1 b_2 - b_1 c_2}{a_1 b_2 - b_1 a_2}$$

$$y = \frac{\begin{vmatrix} a_1 & c_1 \\ a_2 & c_2 \end{vmatrix}}{\begin{vmatrix} a_1 & b_1 \\ a_2 & b_2 \end{vmatrix}} = \frac{a_1 c_2 - a_2 c_1}{a_1 b_2 - b_1 a_2}$$

It is evident that x and y correspond to M_1 and M_2, respectively, in equations (7) and (8), and a and b, to the constants in these equations.

The critical load for an ideal beam-column is that axial load which produces infinite bending moments somewhere along its length; consequently, if the moments over the supports are infinite, it follows that the critical load must have been reached. It is obvious from an inspection of the foregoing expressions that both x and y will be infinite if the denominators of the right-hand terms are zero, provided, of course, that the numerators are not simultaneously equal to zero. This result is not likely and, in fact, may be checked for the condition of

end load which gives a value of zero to the denominator. If c_1 and c_2, which correspond to k_1 and k_2, are zero, the numerators are always zero, regardless of the values of the a and b terms. Therefore both k_1 and k_2 will be zero unless a side load is assumed to act on the beam-column, but with side load acting, regardless of its magnitude, the numerators will be finite unless the a and b terms make them otherwise. Hence it is seen that the quantity of the side load need not be known, but its presence must be assumed.

Equating the denominators to zero, then

$$\begin{vmatrix} a_1 & b_1 \\ a_2 & b_2 \end{vmatrix} = 0$$

Substitution of the corresponding values from equations (7) and (8) gives

$$\begin{vmatrix} 2L_1\beta_1 & L_1\alpha_1 \\ L_1\alpha_1 & (2L_1\beta_1 + 2L_2\beta_2 + L_2\alpha_2) \end{vmatrix} = 0$$

Dividing through by L_1 and expanding

$$4(\beta_1)^2 + 4\beta_1\beta_2 L_2/L_1 + 2\alpha_2\beta_1 L_2/L_1 - (\alpha_1)^2 = 0$$

$$\beta_1(4\beta_1 + 4\beta_2 L_2/L_1 + 2\alpha_2 L_2/L_1) = (\alpha_1)^2 \qquad (9)$$

The quantities α and β are tabulated for various values of L/j on page 212 of reference 3, and the value of L/j that gives values of α and β which satisfy equation (9) will be the critical one.

The determination of the critical value of L/j for the beam-column of figure 10 may be carried out by trial. In this case $L_2 = 2L_1$, $L_2/j_2 = 2L_1/j_1$, and equation (9) becomes

$$\beta_1(4\beta_1 + 8\beta_2 + 4\alpha_2) = (\alpha_1)^2$$

or

$$A\ \beta_1 = (\alpha_1)^2$$

where $A = (4\beta_1 + 8\beta_2 + 4\alpha_2)$

Solving this equation by trial shows that as L_1/j_1 increases from 1.00, the left-hand side goes to positive infinity, changes sign, and increases from negative infinity, becoming practically equal to the right-hand side when $L_1/j_1 = 2.47$. For this case, then, the end load will be critical when $L_a/j_a = 4.94$.

In a similar case with three bays of equal length, $L_2 = L_1$, and since $L_1/j_1 = L_2/j_2$, $\alpha_1 = \alpha_2$ and $\beta_1 = \beta_2$, equation (9) reduces to

$$\beta(8\beta + 2\alpha) = \alpha^2$$

Solving this expression by trial shows that, as L/j increases from 1.00, both sides of equation (9) increase to positive infinity and decrease again with positive sign, always with the left-hand side greater in magnitude than the right until L/j reaches 3.86 when the two sides are practically equal. When $L/j = \pi$, both terms become infinite, but the solution for the moments yields the indeterminate form ∞/∞. For values of L/j greater than π, the moment equations still give consistent values for the moments until $L/j = 3.86$. Hence it appears that 3.86 is the critical value of L/j for this second case.

It is of interest to compare the critical loads for these two cases, as the ratio indicates a theoretical increase in strength due to using end bays only half as long as the critical bay instead of having all bays of the same length. The numerical values of the critical end loads for the two cases are not necessary for this study; only the ratio between them is required, and it may be determined from the critical L/j's. Let subscripts a and b designate quantities for the first and second cases, respectively, and consider only the critical quantities for the central 18-inch spans of the columns. The ratio of the L/j's may be written

$$\text{Ratio} = \frac{L_a/j_a}{L_b/j_b} = \frac{j_b}{j_a}$$

since $L_a = L_b$. The modulus of elasticity E, and the moment of inertia I, are the same for both column sections and, since $j^2 = EI/P$,

$$\frac{j_b}{j_a} = \sqrt{\frac{EI/P_b}{EI/P_a}} = \sqrt{\frac{P_a}{P_b}}$$

The ratio of the critical end loads P, then, may be expressed as

$$\frac{P_a}{P_b} = \left(\frac{L_a/j_a}{L_b/j_b}\right)^2 \qquad (10)$$

The ratio of the critical end loads for the two cases is then found, by substituting in equation (10) the critical values of L/j, to be

$$\frac{P_a}{P_b} = \left(\frac{4.94}{3.86}\right)^2 = 1.64$$

According to this ratio, the cylinder of the first case, which corresponds exactly to cylinder 1, would be expected to carry 64 percent more stress in the compression fiber than the cylinder of the second case. It appears, therefore, that the maximum stress found from test 1 should be reduced in the ratio of 1.00/1.64 to represent fairly the strength of a cylinder with uniform 18-inch bulkhead spacing.

Similar calculations for beam-columns of 1, 2, and 4 equal spans with fixed ends have been made and the critical values of L/j listed in table IV.

The importance of the end conditions may be found by comparing these values with similarly computed values of critical L/j for pin-ended beam-columns with the same arrangements of supports. Such values are also listed in table IV. It will be noted that for all cases of bays of equal length and pin ends, the critical value of L/j is π. For some cases, notably that of two equal bays, the method of computation previously outlined results in computed values of critical L/j in excess of π but, as is explained on page 223 of reference 3, such results presuppose a perfect symmetry of the structure and loading that is never obtained in practice.

In addition to the critical values of L/j, table IV shows the corresponding ratios of critical load P_c, to the Euler load, P_e, at which $L/j = \pi$. For the ideal conditions assumed for this analysis, the Euler formula

$P_e = c\pi^2EI/L^2$, applies, so it may be said that the value of P_c/P_e is the ideal value of restraint coefficient c, which should be indicated by plotting the stress at failure against slenderness ratio, as was done in figure 9.

TABLE IV

IDEAL CRITICAL LOADS

Condition	Critical L/j	P_c/P_e
Three spans, A - 2A - A, fixed ends	4.94	2.47
" " " pinned "	4.49	2.02
n equal spans, pinned ends	3.14	1.00
One span, fixed ends	6.28	4.00
Two equal spans, fixed ends	4.49	2.02
Three equal spans, fixed ends	3.86	1.51
Four equal spans, " "	3.59	1.31

COMPARISON OF INDICATED RESTRAINT COEFFICIENTS

If it is assumed that the values of P_c/P_e of table IV do represent the values of c that should have been indicated by the test results, the following comparison is obtained.

TABLE V

INDICATED RESTRAINT COEFFICIENTS

Condition	Cylinder 1	Cylinder 3
Actuat test	2.68	1.56
Fixed ends	2.47	1.31
Pinned ends	2.02	1.00

A high degree of precision must not be claimed for any of the values of indicated restraint coefficient listed in table V. Those computed from the test data depend on calculated values of stress and slenderness ratio, neither of which are very precise on account, primarily, of the relatively low precision of the measured dimensions of the corrugations and the lack of uniformity between the corrugations. The probable error due to lack of precision in measuring the pitch and depth of a corrugation could be computed, but it would be of little value as the computed radius of gyration depends on the assumption that the corrugated section is made up of a number of true circular arcs tangent to each other at the pitch line. That this assumption is of doubtful validity is indicated by the discrepancy between the equivalent thicknesses computed from the weights of pieces of the material, and those computed from the p/d ratio. Furthermore, the stress values assumed to have been realized in the tests reflect any error in the determination of the equivalent thicknesses. If those computed from the p/d ratio had been used in computing the section moduli, the computed stresses, and therefore the indicated restraint coefficients, would have been higher than those listed in tables III and V. Originally it was hoped to obtain more precise values of the actual stresses developed by taking extensometer measurements during the tests. It was found, however, that these readings were unreliable as the slightest buckling of the material made them meaningless. The values of restraint coefficient listed in table V as having been indicated by the tests must therefore be rated as only approximate.

Similarly the procedure for determining the theoretical values of restraint coefficient that should have been indicated by the test results was such that the resulting figures cannot be considered very precise. Probably the most important source of error was the neglect of the curvature of the pitch line. As previously stated this curvature should increase the strength of the most heavily loaded corrugation, and the tests indicate clearly that it does so, but the data are inadequate in both quantity and quality to provide a quantitative measure of this action.

While the neglect of pitch-line curvature tended to reduce the computed values for indicated restraint coefficient, some of the other assumptions tended to increase them. Most important of these was the assumption of an ideal material with an infinite proportional limit. All practical materials have finite proportional limits above

which the slope of the stress-strain curve diminishes. As a result, the practical critical loads at which failure actually takes place are always less than the ideal critical loads obtained from analyses like that carried out in the foregoing sections. For members of high slenderness ratios, with negligible transverse loads and deflections of intermediate supports, the difference between the ideal and practical critical loads is so small that it may be neglected, but when these conditions are not present the difference may be very large. In the cases under consideration, the fact that the stresses at failure came within the range of the straight-line formula shows that the differences between the two critical loads would be appreciable. The bending of the cylinder causing the supports of a corrugation to fall on a curved line and the ends to rotate with respect to each other would make this difference greater than would be the case if the actual conditions of support had been the same as those assumed for the analysis.

The assumption of a constant axial load also would tend to increase the theoretical values of indicated c. In reference 4, James shows that the stiffness of a beam-column decreases at an accelerating rate as L/j increases. Thus the decrease in stiffness, and hence the restraint on the critical bay due to the greater load on the adjacent inboard panel, is greater than the increase due to the smaller loads on the outboard panels. Therefore the critical values of L/j in table V are somewhat larger than those which would have been obtained from analyses in which the variation in axial load was taken into account.

The primary objective of the foregoing analysis to determine the critical load of a corrugation was to determine how closely the effect of variations in the lengths of bays on the general instability stress of the cylinder covering could be predicted. Owing to the causes mentioned, the values listed in table V are not sufficiently precise to permit precise quantitative conclusions on this point. It is believed, however, that they justify the statement that valuable qualitative conclusions as to the effect of varying the lengths of bays can be obtained from analyses of this type.

In the application of the results of the cylinder tests to practical fuselage design, it should be remembered that the end rings to which the cylinders were attached were relatively much stiffer than the bulkhead rings

or frames likely to be used in an airplane. Until further tests justify a less conservative procedure, it is recommended that where the bulkhead rings or frames are equally spaced, the design be made on the assumption that the most stressed corrugation is a pin-ended column with a length equal to that between frames. For the present, therefore, the type of critical load analysis just illustrated is of more value for the interpretation of tests than for computing stresses to be allowed in design.

Attention should be directed to the necessity of knowing the actual dimensions of any corrugated sheet used in the primary structure of an airplane. The first study of the cylinder tests was made on the assumption that the nominal dimensions of the corrugations were correct. The result was that the indicated values of restraint coefficient were only $c = 1.69$ for cylinder 1 and $c = 1.02$ for cylinder 3. Both of these values are considerably below the figures for fixed-end conditions listed in table V. The value for cylinder 1 is even below that for the pin-ended condition, while that for cylinder 3 is not significantly above that for the pin-ended condition. In the foregoing analysis for the determination of critical loads, it was found that, theoretically, cylinder 1 should carry 1.64 times as much as a similar cylinder with three 18-inch bays. On this basis it appeared that test 1 indicated the restraint coefficient for a cylinder with three 18-inch bays would have been only $1.69/1.64 = 1.03$, or practically the same as for cylinder 3. As these results suggested that neither the restraint at the ends of the cylinders nor the pitch-line curvature increased the general instability stress of the corrugated cylinder covering, the tests were considered of little practical value. The later study based on the corrected values for the corrugation dimensions was needed to demonstrate their real worth. It is true that the design recommendations of the preceding paragraph are practically the same as those drawn from the earlier study of the data, but they are now made with the knowledge that they are conservative and subject to liberalization as more test data is accumulated; whereas they were hardly justified on the basis of the earlier study.

REMARKS ON BULKHEAD RINGS

One of the most important problems of fuselage design is the determination of the stiffness and strength required

in the bulkhead rings to permit them to act as effective supports to the corrugations of the skin. In some earlier editions of Department of Commerce Bulletin 7-A the rule was laid down that each bulkhead ring should be designed to carry as a column a load equal to the shear on the section, the unsupported length being assumed as not less than half the height of the ring. The rings used in the test cylinders under discussion were of the same size as those in the cylinder tests reported by Mossman and Robinson in reference 2. In that report the strength of a ring computed according to the Department of Commerce rule was only 696 pounds. In the tests under discussion the maximum shear of 8,260 pounds caused no noticeable distortion of the rings. This result shows the excessive severity of the earlier Department of Commerce rule, which has now properly been abandoned. Unfortunately, the tests give no indication as to how much lighter the rings might have been without losing their effectiveness as supports to the skin.

Although the tests under consideration fail to show how light the bulkhead rings may be made, they indicate clearly the advantage of using a large number of light rings closely spaced, instead of a small number of relatively heavy rings. If it is assumed, as suggested, that cylinder 2 would have carried the same load as cylinder 3 if the rivets had been perfect, it is seen that the mere addition of a light bulkhead ring in the middle of the 18-inch panel of cylinder 1 resulted in an increase of stress from 18,100 to 28,400 pounds per square inch. Thus a 7.5-percent increase in weight of specimen gave a 57-percent increase in stress at failure, and 46-percent improvement in strength-weight ratio.

CONCLUSIONS

The following conclusions may reasonably be drawn from the cylinder tests under consideration:

1. When failure occurs by bending of the corrugations normal to the skin, the computed stress on the extreme fiber of a corrugated cylinder is in excess of that for a flat panel of the same basic pattern and panel length tested as a pin-ended column.

2. The added strength is due to the effects of curvature of the pitch line.

3. There is, as yet, insufficient data to determine quantitatively the increase in strength resulting from pitch-line curvature.

4. The effect of varying the distance between transverse supports (bulkhead rings or frames) can be determined qualitatively by analyses of the type illustrated in the discussion.

5. Deviations of the actual dimensions from the nominal in commercial corrugated material are likely to be of appreciable magnitude, and in design it is advisable to determine with care the actual dimensions of the material to be used.

6. In practical design it is desirable to neglect the strengthening effect of pitch-line curvature and restraint at heavy bulkheads until more test data indicates the extent to which these factors can be relied upon.

7. Where bulkheads and frames are light and equally spaced it is advisable to assume the length equal to the bulkhead spacing and the restraint coefficient equal to unity.

8. A large number of light bulkhead frames will be more efficient than a small number of relatively heavy ones. The heavy bulkheads should be used only where the structure is subjected to heavy concentrated loads, as at the wing reactions.

9. More test data is needed on the problem of the stiffness required in the bulkheads.

10. More test data is desirable to determine qualitatively the strengthening effect of pitch-line curvature.

Guggenheim Aeronautic Laboratory,
Stanford University, California,
January 20, 1937.

REFERENCES

1. Greene, C. F., and Brown, C. G.: The Column Properties of Corrugated Aluminum Alloy Sheet. A.C.I.C. No. 699, Matériel Division, Army Air Corps, 1935.

2. Mossman, Ralph W., and Robinson, Russell G.: Bending Tests of Metal Monocoque Fuselage Construction. T.N. No. 357, N.A.C.A., 1930.

3. Niles, A. S., and Newell, J. S.: Airplane Structures. John Wiley & Sons, Inc., 1929.

4. James, Benjamin Wylie: Principal Effects of Axial Load on Moment-Distribution Analysis of Rigid Structures. T.N. No. 534, N.A.C.A., 1935.

APPENDIX I

DERIVATION OF EQUATIONS FOR THE PROPERTIES OF CORRUGATED SHEET

The properties for which formulas are now derived are those of a series of tangent circular arcs, each multiplied by a thickness t. Though the results are not strictly applicable to sections of corrugated sheet, the resulting error is much less than that due to the variation of commercial sheet from its theoretical dimensions. The nomenclature and dimensions used are indicated in figure A-1.

1. Area of one arc:

$$A = \int t\, ds = 2 \int_0^{\theta} t\, r\, d\alpha = 2t\, r\, \theta \qquad (A1)$$

2. Moment of inertia of one arc about the pitch line.

$$I = \int \left(\frac{d}{2} - y\right)^2 t\, ds = 2 \int_0^{\theta} \left(\frac{d}{2} - y\right)^2 t\, r\, d\alpha$$

$$= 2 \int_0^{\theta} \left[(r - r\cos\theta) - (r - r\cos\alpha)\right]^2 t\, r\, d\alpha$$

$$= 2t\, r^3 \int_0^{\theta} (\cos\alpha - \cos\theta)^2\, d\alpha$$

$$= 2t\, r^3 \int_0^{\theta} (\cos^2\alpha - 2\cos\alpha\cos\theta + \cos^2\theta)\, d\alpha$$

$$= 2t\, r^3 \left[\frac{\alpha}{2} + \frac{1}{4}\sin 2\alpha - 2\sin\alpha\cos\theta + \alpha\cos^2\theta\right]_0^{\theta}$$

$$I = 2t\, r^3 \left[\theta\left(\frac{1}{2} + \cos^2\theta\right) - \frac{3}{4}\sin 2\theta\right] \qquad (A2)$$

3. Radius of gyration of one arc about the pitch line.

$$\rho = \frac{I}{A} = \sqrt{\frac{2t\, r^3 \left[\theta\left(\frac{1}{2} + \cos^2\theta\right) - \frac{3}{4}\sin 2\theta\right]}{2t\, r\theta}}$$

$$\rho = r\sqrt{\frac{1}{2} + \cos^2\theta - \frac{3}{4}\frac{\sin 2\theta}{\theta}} \qquad (A3)$$

4. Included angle of one-half of an arc in terms of pitch and radius of corrugation.

By inspection

$$\sin \theta = \frac{p}{4} \frac{1}{r} = \frac{p}{4r}$$

$$\theta = \sin^{-1} \frac{p}{4r} \tag{A4}$$

5. Radius of corrugation in terms of pitch and depth.

By inspection $r (1 - \cos \theta) = d/2$

$$r \left(1 - \sqrt{1 - \sin^2 \theta}\right) = d/2$$

$$r \left[1 - \sqrt{1 - \left(\frac{p}{4r}\right)^2}\right] = \frac{d}{2}$$

$$\sqrt{1 - \left(\frac{p}{4r}\right)^2} = 1 - \frac{d}{2r}$$

$$- \frac{p^2}{16r^2} = \frac{d^2}{4r^2} - \frac{d}{r}$$

$$p^2 = 16r\,d - 4d^2$$

$$r = \left[\frac{p^2}{16d^2} + \frac{1}{4}\right] d \tag{A5}$$

6. Moment of inertia per inch of pitch line.

I per inch of pitch line =

$$= \frac{2t\, r^3 \left[\theta \left(\frac{1}{2} + \cos^2 \theta\right) - \frac{3}{4} \sin 2\theta\right]}{p/2}$$

7. Ratio of weight of corrugated sheet to weight of flat sheet of same thickness and projected area.

$$\varphi = \frac{2r\,\theta}{0.5\,p} = \frac{4r\theta}{p} \tag{A6}$$

8. Summary of formulas.

The foregoing formulas may be written:

$$r = k_1 d \tag{A7}$$

where $$k_1 = \frac{1}{4}\left[\frac{1}{4}\left(\frac{p}{d}\right)^2 + 1\right] \tag{A7a}$$

$$\rho = k_2 d \tag{A8}$$

where $$k_2 = k_1 \sqrt{\frac{1}{2} + \cos^2 \theta - \frac{3}{4}\frac{\sin 2\theta}{\theta}} \tag{A8a}$$

$$I = k_3 t \frac{d^3}{p} \text{ per inch of pitch line} \tag{A9}$$

where $$k_3 = 4k_1^3 \left[\theta\,(0.5 + \cos^2 \theta) - \frac{3}{4}\sin 2\theta\right] \tag{A9a}$$

$$\varphi = 4k_1 d \frac{\theta}{p} = \frac{4k_1 \theta}{(p/d)} \tag{A10}$$

Values of k_1, k_2, k_3, and φ are listed in table A-1 and are plotted against p/d in figures A-1 and A-2.

TABLE A-1

COEFFICIENTS FOR PROPERTIES OF CORRUGATED SHEET

p/d	k_1	k_2	k_3	φ	θ
2.0	0.5000	0.3536	0.3927	1.5708	1.5708
2.5	.6406	.3568	.4401	1.3832	1.3495
3.0	.8125	.3589	.4922	1.2740	1.1760
3.5	1.0156	.3603	.5476	1.2052	1.0383
4.0	1.2500	.3613	.6053	1.1591	.9273
4.5	1.5156	.3620	.6647	1.1269	.8364
5.0	1.8125	.3626	.7254	1.1035	.7610
6.0	2.5000	.3633	.8495	1.0725	.6435
7.0	3.3125	.3638	.9760	1.0536	.5566
8.0	4.2500	.3641	1.1042	1.0412	.4900
9.0	5.3125	.3643	1.2335	1.0326	.4373

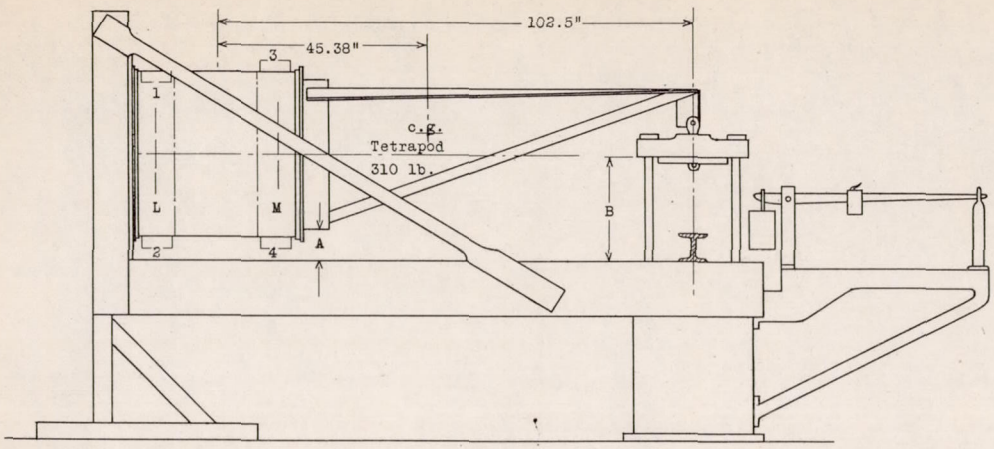

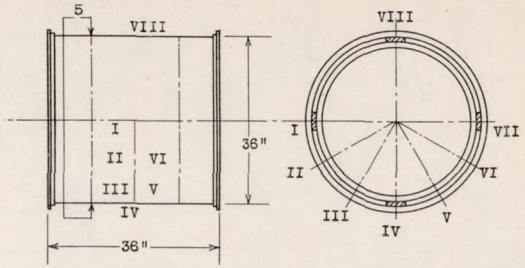

* Arm to section where failure occured. † $\frac{310 \times 45.38}{102.5}$ = 137 lb. equiv. load at apex.

All differences with (+) sign are elongations, (-) signs, contractions.

Run	Load increment	Arm of load increment	Moment increment	Total shear	Total moment	Equiv. load at apex to give total moment	Extensometer readings								Diameter gage 5		Beam deflection				Remarks
							No. 1	Difference	No. 2	Difference	No. 3	Difference	No. 4	Difference			Distance A		Distance B		
	lb.	in.	in.-lb.	lb.	in.-lb.	lb.	in.		in.		in.		in.		in.	difference	in.	difference	in.	difference	
1	310	* 45.38	14080	310	14080	† 137	.1492	10	.0216	-10	.1565	03	.0097	-08	.0290	05	14.80	0	21.85	03	
2	255	102.5	26150	565	40230	392	.1482	13	.0226	13	.1562	05	.0105	10	.0295	02	14.80	0	21.82	03	
3	260	↑	26650	825	66880	652	.1469	13	.0239	10	.1557	05	.0115	10	.0297	-02	14.80	0	21.75	07	
4	225		23050	1050	89930	877	.1456	13	.0249	13	.1552	05	.0125	12	.0295	23	14.80	0	21.70	05	
5	270		27650	1320	117580	1147	.1443	08	.0262	11	.1546	06	.0137	17	.0318	27	14.77	03	21.65	05	Very slight bulging outward at IV.
6	240		24600	1560	142180	1387	.1435	20	.0273	15	.1541	05	.0154	13	.0345	15	14.75	02	21.57	08	No change.
7	255		26150	1815	168330	1642	.1415	14	.0288	14	.1535	06	.0167	20	.0360	30	14.75	0	21.51	06	No change.
8	245		25100	2060	193430	1887	.1401	14	.0302	14	.1529	06	.0187	19	.0390	100	14.73	02	21.46	05	Slight increase in bulge at IV. Faint bulge at III.
9	250		25600	2310	219030	2137	.1387	12	.0316	14	.1522	07	.0206	13	.0490	-60	14.72	01	21.40	06	No change.
10	245		25100	2555	244130	2382	.1375	01	.0332	16	.1516	06	.0219	18	.0430	60	14.72	0	21.35	05	No change.
11	260		26650	2815	270780	2642	.1374	23	.0350	18	.1511	05	.0237	18	.0490	60	14.71	01	21.29	06	Slight increase in bulge at III. No change elsewhere.
12	195		20000	3010	290780	2837	.1351	0	.0363	13	.1509	02	.0247	10	.0490	0	14.70	01	21.25	04	" " " " " " " " " "
13	200		20500	3210	311280	3037	.1351	10	.0375	12	.1504	05	.0257	10	.0490	0	14.70	0	21.20	05	" " " " " " " " " "
14	305		31250	3515	342530	3342	.1341	22	.0393	18	.1498	06	.0277	20	.0510	20	14.67	03	21.11	09	No change.
15	195		20000	3710	362530	3537	.1319	9	.0402	09	.1494	04	.0287	10	.0520	10	14.67	0	21.06	05	No change.
16	200		20500	3910	383030	3737	.1310	11	.0415	13	.1491	03	.0305	18	.0530	10	14.66	01	21.01	05	No change.
17	220		22550	4130	405580	3957	.1299	06	.0429	14	.1487	04	.0318	13	.0550	20	14.65	01	20.94	07	Slight increase in bulge at III. Faint bulge at V.
18	185		18970	4315	424550	4142	.1293	09	.0442	13	.1483	03	.0333	15	.0570	20	14.64	01	20.88	06	No change
19	195		20000	4510	444550	4337	.1284	01	.0455	17	.1480	03	.0348	15	.0560	-10	14.63	01	20.84	04	Slight increase in bulges at III, IV, and V.
20	185		18970	4695	463520	4522	.1283	13	.0472	30	.1477	04	.0367	19	.0550	-10	14.62	01	20.79	05	Slight increase at III, IV, V. Notice scale beam drops 10 lb. during reading.
21	205		21000	4900	484520	4727	.1270		.0502		.1473		.0406	-39	.0520	-30	14.61	01	20.72	07	Rather rapid increase in bulge at V.
22	200		20500	5100	505020	4927													20.65	07	Bulges between III and V were about .25 in. deep.
23	200		20500	5300	525520	5127	← gages removed →														Maximum load. Gradual increase in bulges around bottom and up both sides. Scale beam dropped 60 lb.
24	1320	↓ 102.5	-135300	3980	390220	3807											14.47	14	19.84	81	Nodes of corrugations at IV start to crumple. Maximum depth of bulge is 1.67 in.

With all variable load off, specimen sprang back to a position such that distance B = 21.25" or 60" less than original position.
Second maximum equivalent load at apex = 3,477 lb. Distance B = 19.47 in. Total deflection at B = 21.85 - 19.47 = 2.38 in.
Percentage of first maximum load = $(\frac{3477}{5127}) \times 100$ = 67.8 percent. Log sheet of test 1 - cylinder with 18-inch ring spacing.

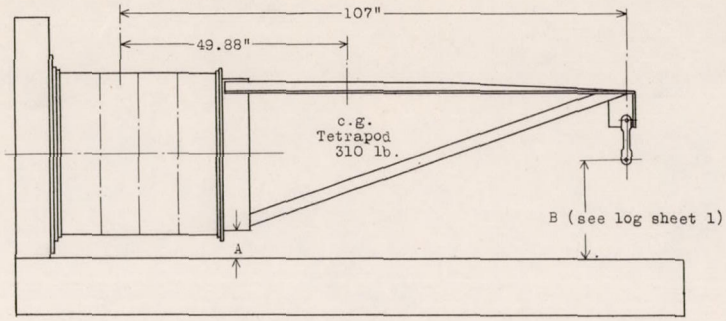

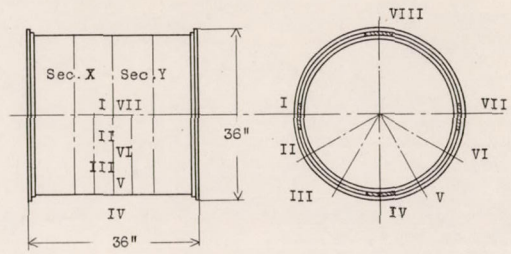

* Arm to section where failure occured. † $\frac{310 \times 49.88}{107}$ = 145 lb. equiv. load at apex.

All differences with (+) signs are elongations, (−) signs contractions.

Run	Load increment	Arm of load increment	Moment increment	Total shear	Total moment	Equiv. load at apex to give total moment	Extensometer readings								Diameter gage 5	Beam deflection				Remarks
							No. 1	Difference	No. 2	Difference	No. 3	Difference	No. 4	Difference		Distance A		Distance B		
	lb.	in.	in.-lb.	lb.	in.-lb.	lb.	in.		in.		in.		in.		difference in.	in.	difference	in.	difference	
1	310	* 49.88	15463	310	15463	† 145										14.86	01	22.10	14	Faint initial bulges, in at III and out at V.
2	560	107	59920	870	75380	605										14.85	04	21.96	06	
3	475	↑	50825	1345	126205	1180										14.81	02	21.90	05	
4	485		51895	1830	178100	1665										14.79	01	21.85	15	
5	480		51360	2310	229460	2145										14.78	02	21.70	11	
6	480		51360	2790	280820	2625										14.76	02	21.59	16	
7	545		58315	3335	339135	3170										14.74	03	21.43	10	
8	480		51360	3815	390495	3650										14.71	02	21.33	08	
9	490		52430	4305	442925	4140										14.69	02	21.25	12	
10	525		56175	4830	499100	4665										14.67	02	21.13	14	Slight bulge out at III and in at V (sec. X)
11	500		53500	5330	552600	5165										14.65	03	20.99	09	Bulge increased slightly as load increased.
12	460		49220	5790	601820	5625										14.62	03	20.90	15	" " " " " "
13	520		55640	6310	657460	6145										14.59	02	20.75	05	" " " " " "
14	520		55640	6830	713100	6665										14.57	02	20.70	20	" " " " " "
15	450		48150	7280	761250	7115										14.55	04	20.50	10	" " " " " "
16	510		54570	7790	815820	7625										14.51	03	20.40	20	" " " " " "
17	455		48685	8245	864505	8080										14.48		20.20		Large bulges at same points. Load dropped to 8,140 lb.
18	15		1605	8260	866110	8095														Failed.
19				8410	868163	8245														Load held after break.
20																14.77		21.65		Load off.
21		107		8410	868163	8245														Load applied after first load had been taken off.

Second maximum equivalent load at apex = 8,245 lb. Total deflection at B = 22.10 − 20.20 = 1.90 in. Log sheet of test 3 − cylinder with 9-inch ring spacing.

Percentage of first maximum load = $(\frac{8245}{8095})$ x 100 = 72.2 percent.

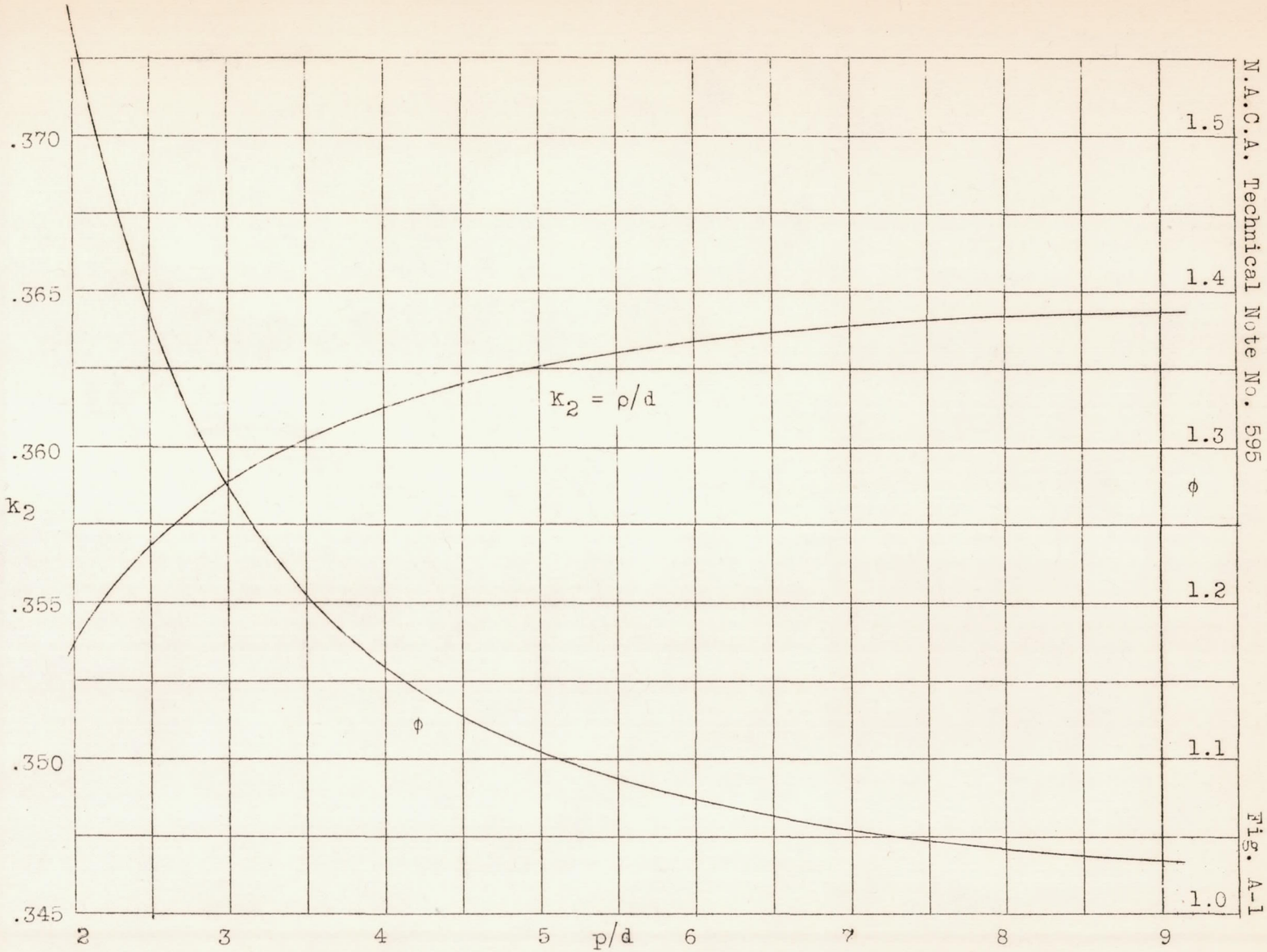

Figure A-1.- Values of ϕ and k_2 for corrugated sheet.

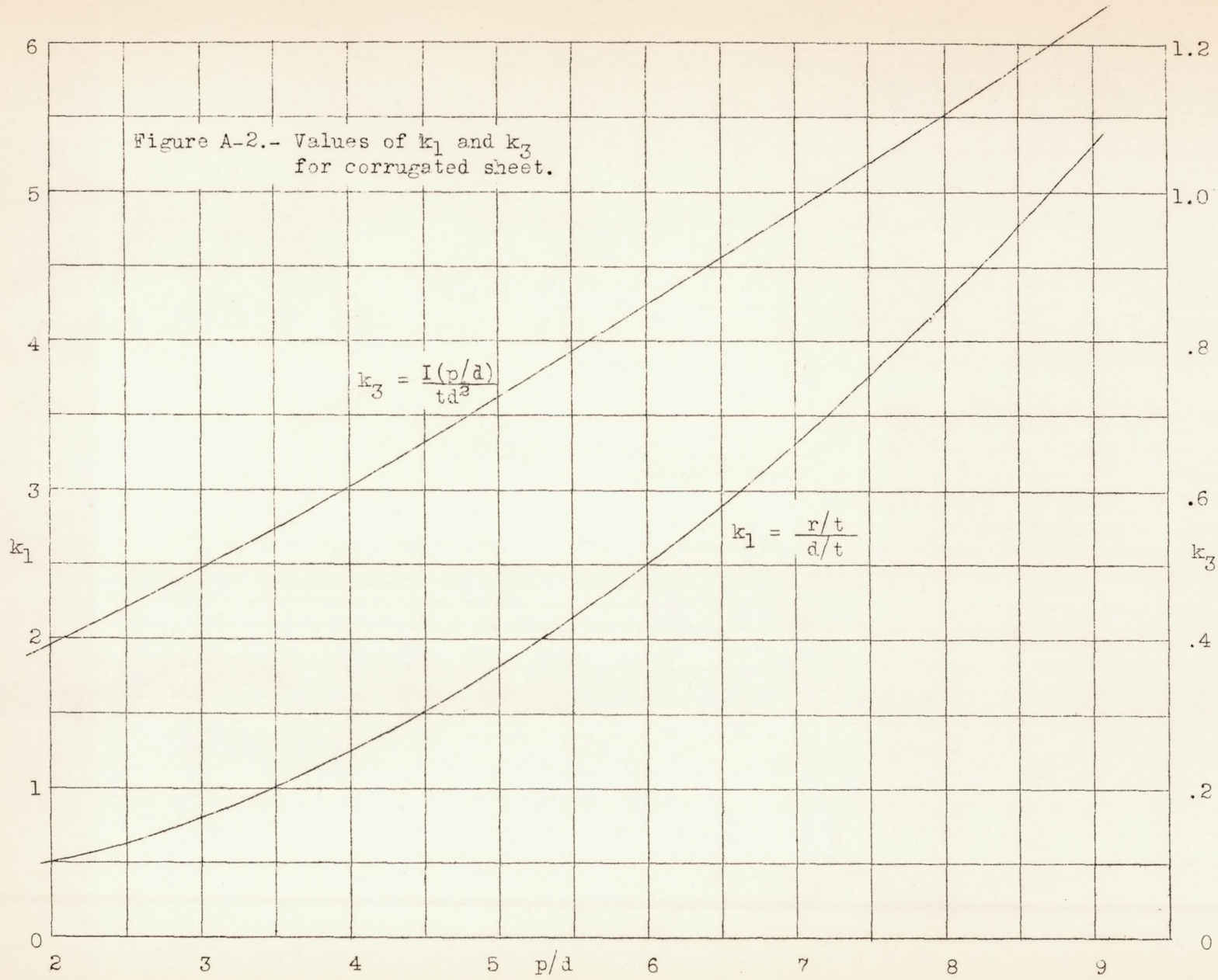

Figure A-2.- Values of k_1 and k_3 for corrugated sheet.

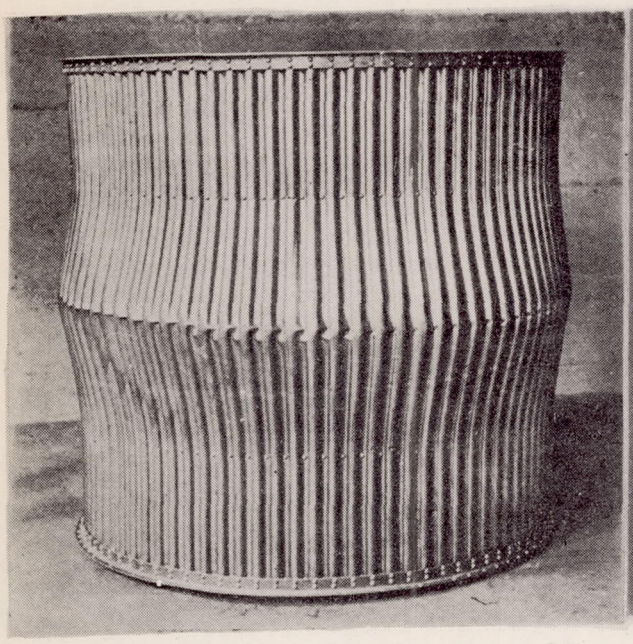

(a)

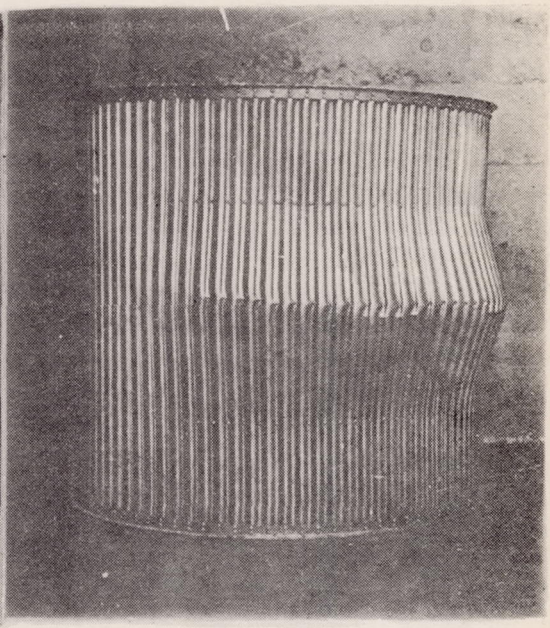

(b)

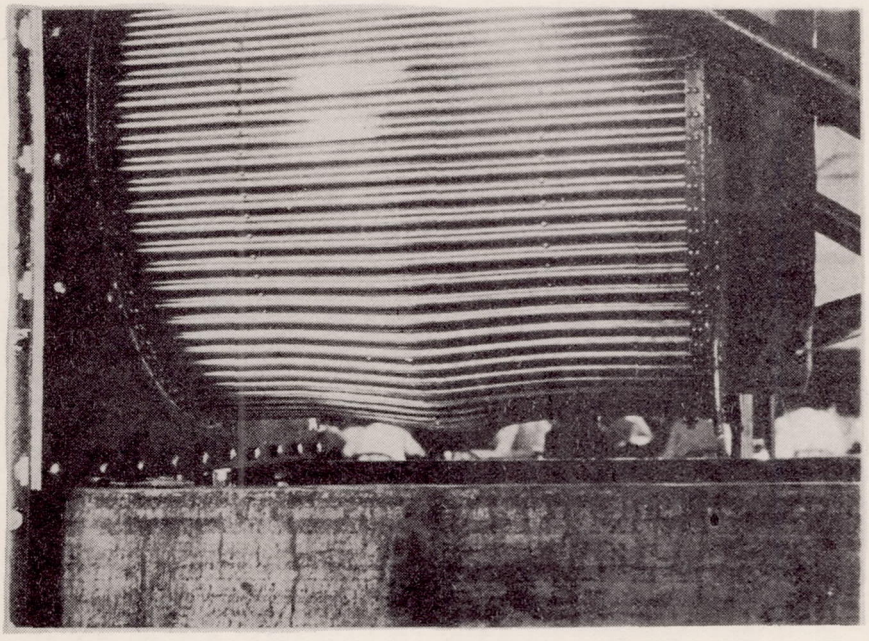

(c)

Figure 1.- Cylinder 1 after failure.

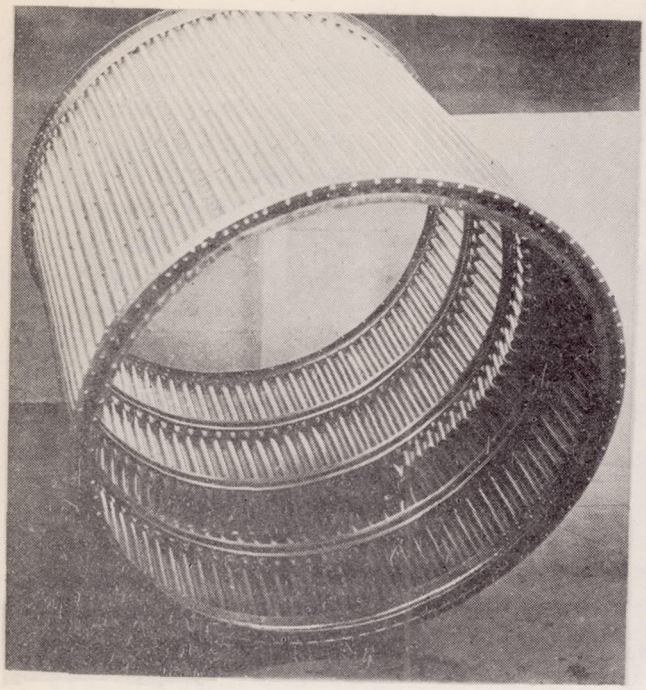

(a)

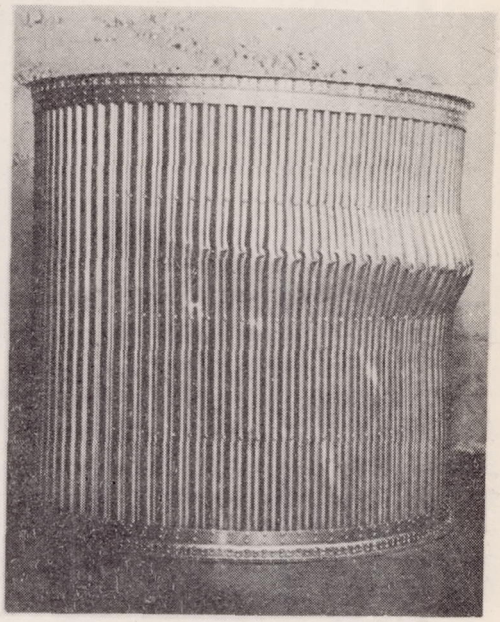

(b)

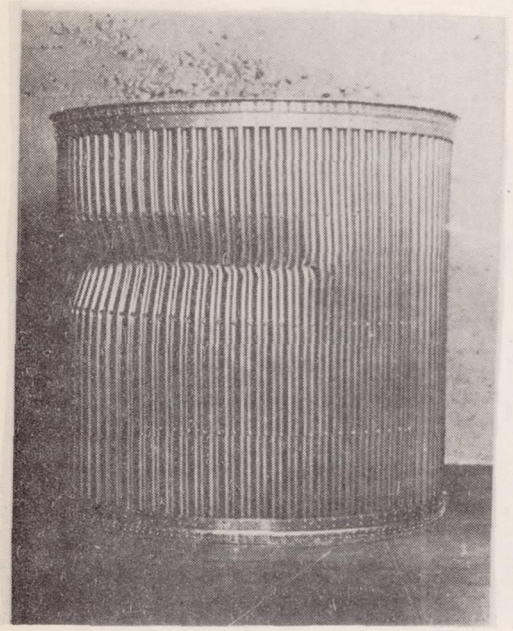

(c)

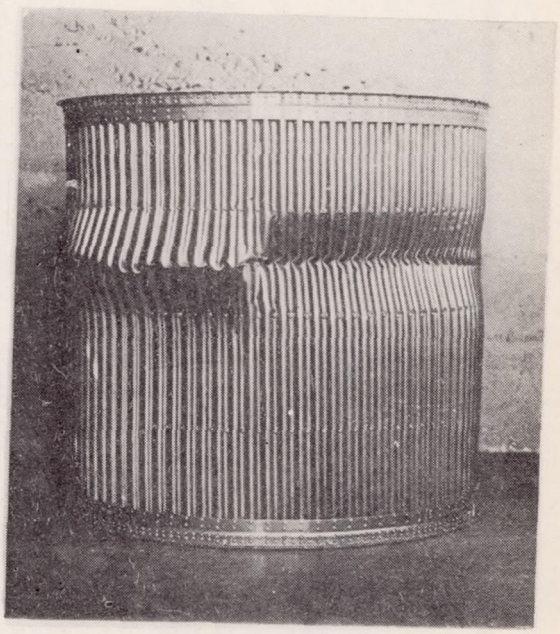

(d)

Figure 2.- Cylinder 3 after failure.

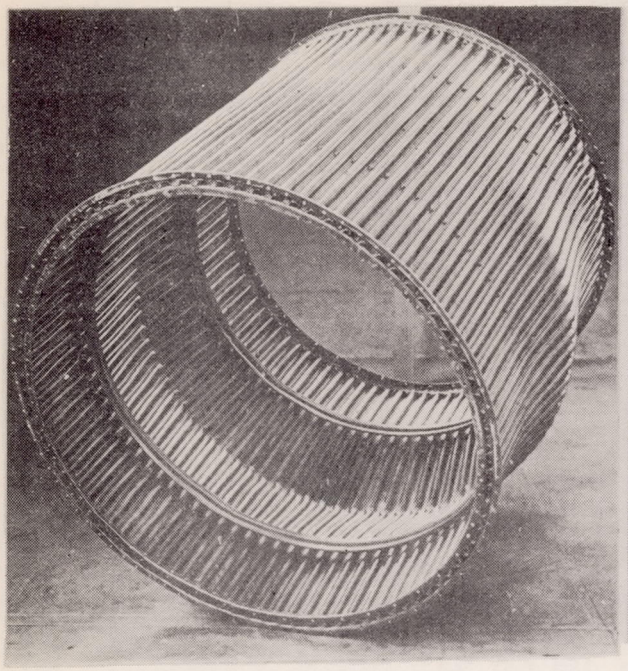

Figure 3.- Failure of cylinder 1.

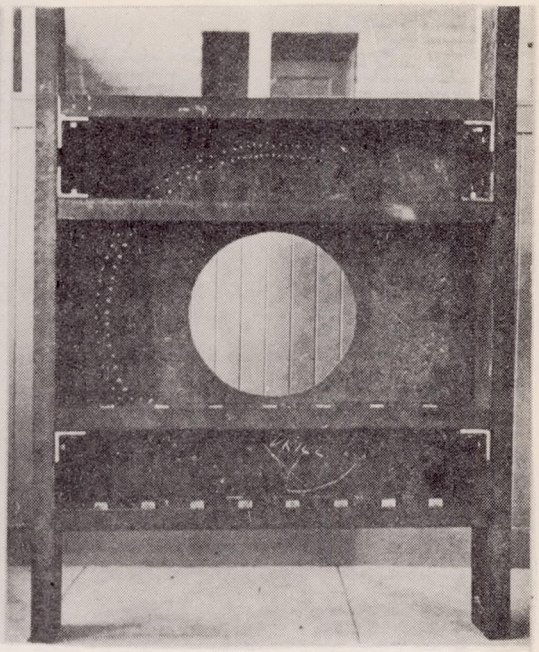

Figure 8.- Backplate of testing jig.

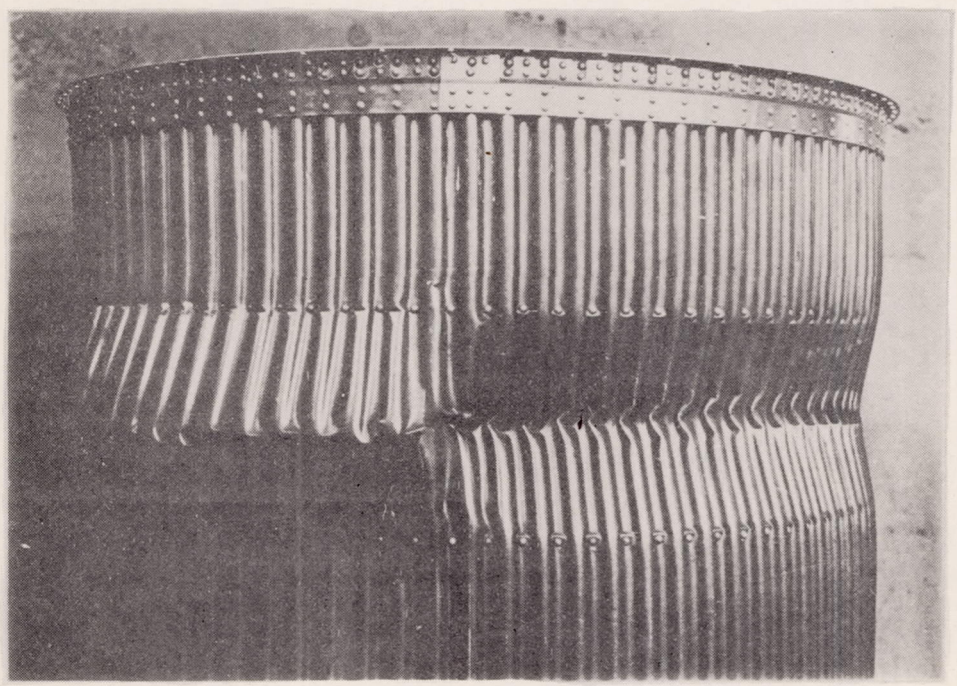

Figure 4.- Failure of cylinder 3.

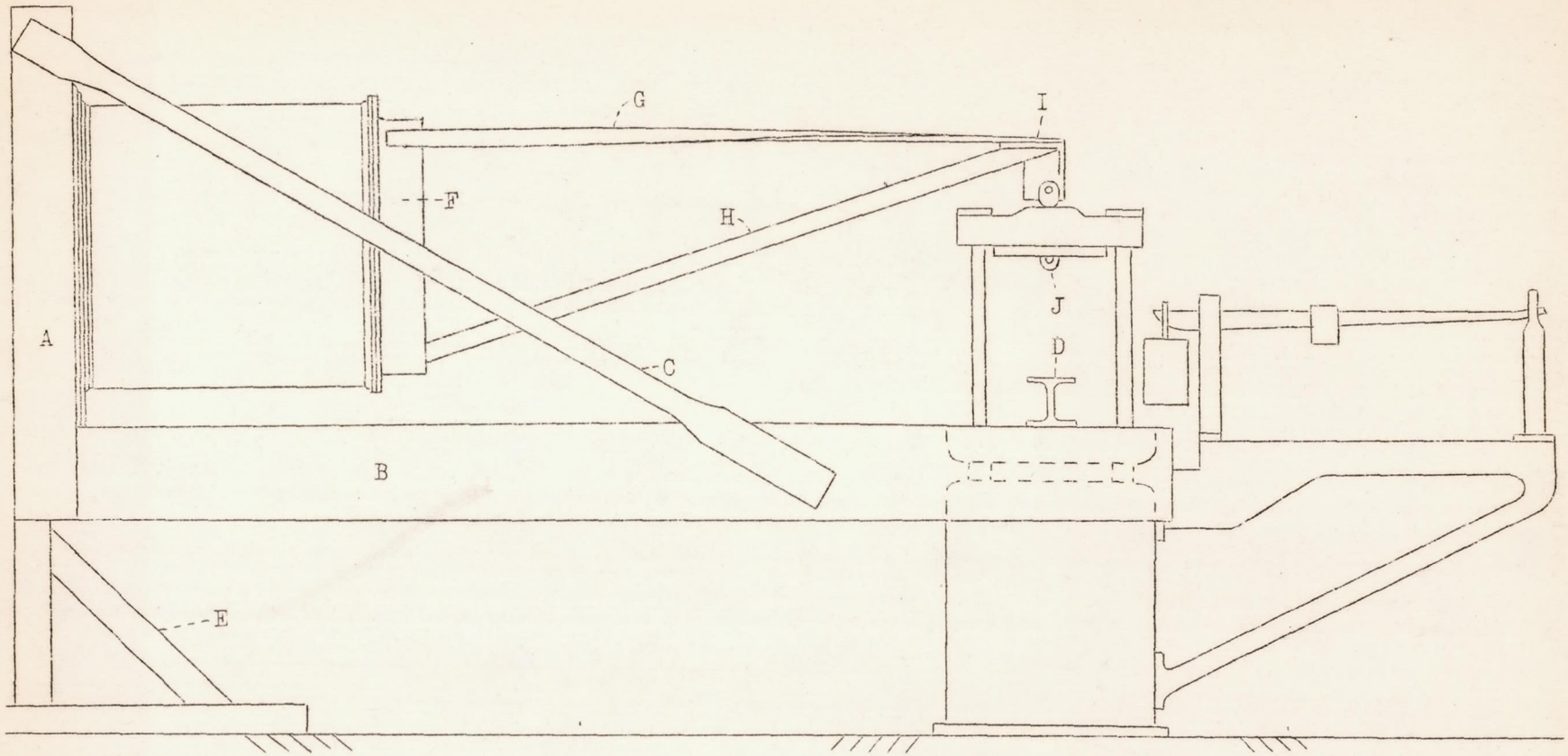

A, 5/8 in. boiler plate stiffened with 8 in. 11.5 lb. channels.
B, 12 in, 20.7 lb. channels.
C, 3 in. conduit pipe.
E, 4 by 4 in. pine.
D, 6 in. 22.8 lb. H-beam.
F, 7 by $3\frac{1}{2}$ by 5/8 in. 21.0 lb. unequal angle.
G, 3 by 1/2 in. flat steel bar.
H, $2\frac{1}{2}$ in. conduit pipe.
J, Milled steel coupling.

Figure 5.- Diagram of test set-up.

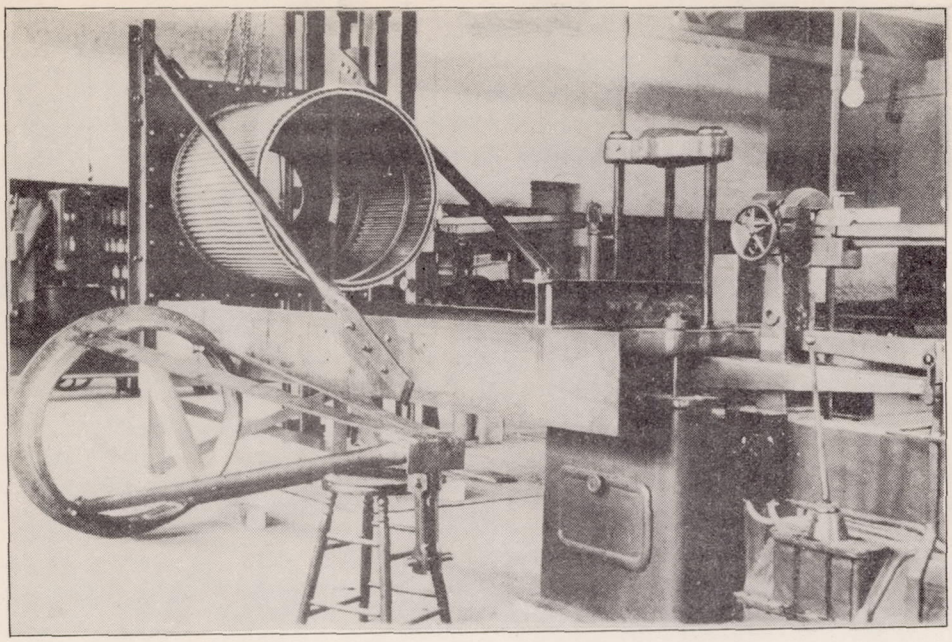

Figure 6.- Testing jig partly assembled.

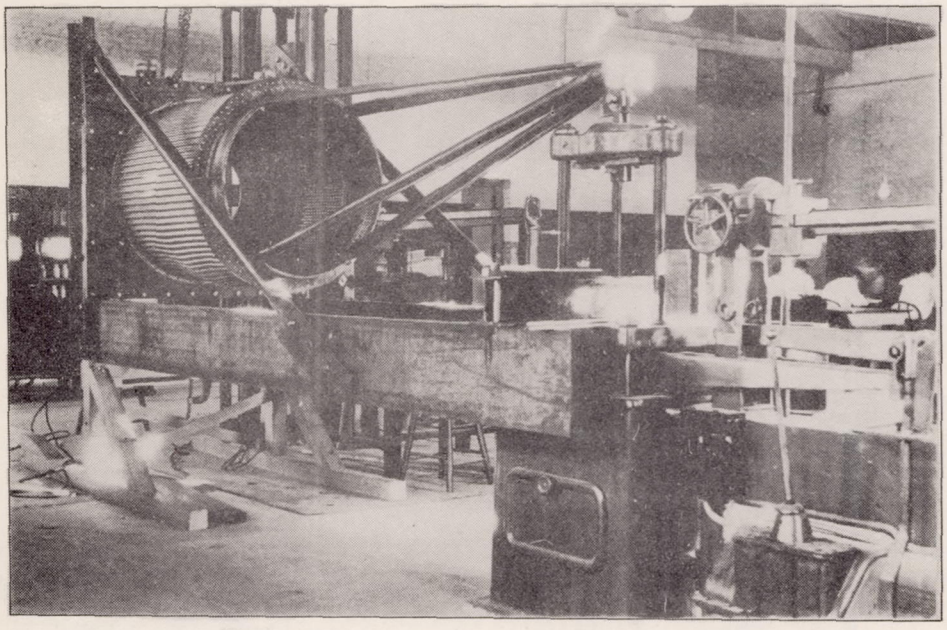

Figure 7.- Cylinder 1 in jig ready for test.

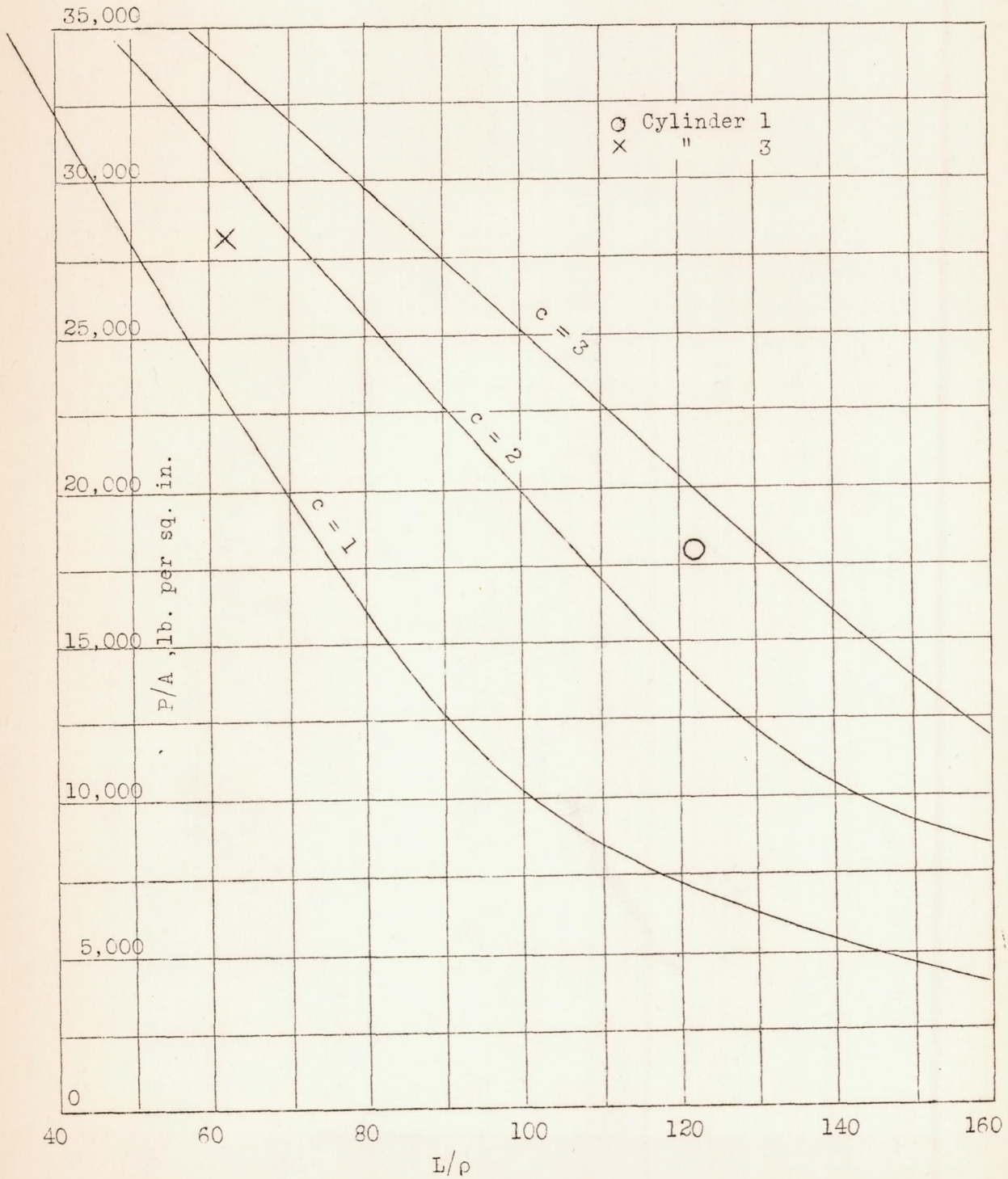

Figure 9.- Relation between column curve and observed stresses at failure.

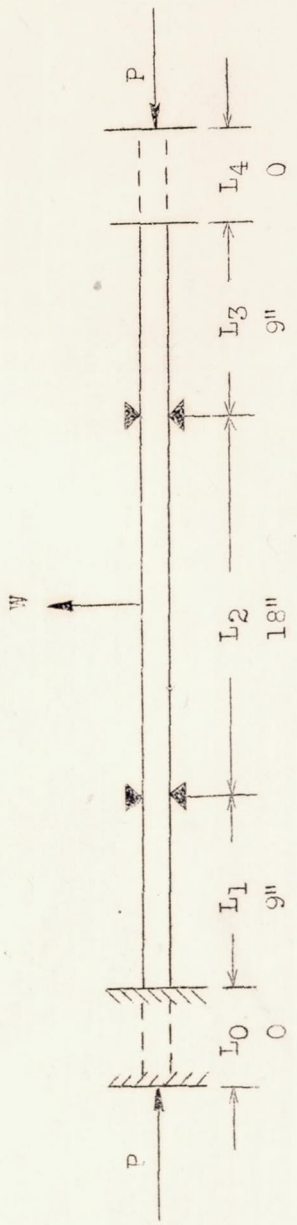

Figure 10.- Loading of assumed beam-column.